Proceedings of the ASME 2025 20th International Manufacturing Science and Engineering Conference
MSEC2025
June 23-27, 2025, Greenville, South Carolina

MSEC2025-155352

LINEAR VOLUMETRIC 3D PRINTING: DUAL-WAVELENGTH INITIATION AND INHIBITION FOR LIGHT-INDUCED DIRECT GROWTH

Yizhen Zhu
School for Engineering of Matter, Transport and Energy, Arizona State University, Tempe, AZ

Shah Md Ashiquzzaman Nipu
School of Manufacturing Systems and Networks, Arizona State University, Mesa, AZ

Parimal Prabhudesai
School for Engineering of Matter, Transport and Energy, Arizona State University, Tempe, AZ

Sheefali Ajay Balapure
School for Engineering of Matter, Transport and Energy, Arizona State University, Tempe, AZ

Xiangjia Li
School for Engineering of Matter, Transport and Energy, Arizona State University, Tempe, AZ

ABSTRACT

This study introduces an advanced volumetric additive manufacturing (AM) method, named light-induced direct growth (LIDG), which leverages dual-wavelength photoinitiation and inhibition to push the boundaries of printing complexity. Traditional vat photopolymerization is valued for its high precision in producing detailed polymer structures, yet it is challenged by the need to balance speed and resolution, the reliance on support structures for complex geometries, and issues with material stability during the fabrication process. The volumetric LIDG technique effectively addresses these limitations through the innovative use of dual-wavelength light sources: blue light initiated photopolymerization, while UV light provides selective inhibition. This dual-wavelength system enables targeted polymerization, allowing for the rapid fabrication of complex, overhanging structures without additional support, thus significantly enhancing the efficiency of the printing process. Additionally, this study explores refined resin formulations and optimized curing methods, which contribute to improved stability and uniformity of the printed materials. These advancements make the LIDG method particularly well-suited for applications in fields that demand high precision and material integrity, such as optics, medical implants, and soft robotics. Overall, the LIDG approach with dual-wavelength control represents a substantial breakthrough in volumetric AM, overcoming the inherent constraints of conventional methods and enabling the faster, more accurate production of intricately detailed components across a range of applications.

Keywords: Additive manufacturing; volumetric printing; dual wavelength; photopolymerization, inhibition

NOMENCLATURE

AM	additive manufacturing
LIDG	light-induced direct growth
VPP	vat photopolymerization
DW-LIDG	dual-wavelength light-induced direct growth
UV	ultraviolet
CQ	camphorquinone
EDAB	ethyl 4-dimethylaminobenzoate
TEGDMA	triethylene glycol dimethacrylate
Bis-GMA	bisphenol A glycerolate dimethacrylate
o-CI-HABI	o-Chloro-4-isocyanatobenzene
THF	tetrahydrofuran

1. INTRODUCTION

Additive manufacturing (AM), or 3D printing, has become a transformative technology in multiple industries, enabling the layer-by-layer creation of complex geometries that were previously difficult or unfeasible to achieve with conventional manufacturing methods [1-3]. AM was initially developed in the 1980s and has since progressed due to advancements in material science, software, and hardware [4,5]. This process facilitates the direct production of components from digital models, reducing material waste and enabling customization and rapid prototyping. Applications of AM encompass various domains, such as aerospace [6,7], biomedical [8-10], automotive [11,12], and micro/nano manufacturing [13-15], due to its capability for precise control over structural and material composition. Direct writing, stereolithography (SLA), inkjet printing, fused

deposition modeling (FDM), and selective laser sintering (SLS) are among the most popular 3D printing methods used extensively for fabrication processes [5]. However, these traditional AM processes encounter challenges, including restricted material selections, reduced production velocities, and difficulties in maintaining consistent quality, particularly in the context of high-precision or multi-material components [16,17]. Moreover, factors such as residual stress, anisotropy, and restricted scalability frequently impede the complete realization of AM in industrial contexts [18]. Researchers are investigating novel approaches to address these limitations, including bio-inspired designs and functional materials at micro and nano scales.

Continuous vat photopolymerization (VPP) signifies a notable progress in AM, addressing the constraints associated with conventional layer-based 3D printing methods [19]. Conventional SLA involves the layer-by-layer curing of photopolymer resins to construct objects, which experience low printing speeds and the presence of visible layer lines, which can detract from both the structural integrity and aesthetic quality of the final product [20,21]. This layer-by-layer method necessitates regular recoating procedures to restore resin between layers, thereby increasing the time and complexity of the fabrication process. To tackle these challenges, methods such as Continuous Liquid Interface Production (CLIP) have been developed, facilitating continuous printing by establishing a "dead zone" at the interface between the resin and an oxygen-permeable window [22,23]. The dead zone inhibits polymerization in that area, facilitating continuous layer formation without adhesion to the base. Nonetheless, despite the capabilities of CLIP, there are persistent geometric and speed constraints, especially concerning complex or extensive structures [24]. Volumetric printing techniques have emerged to further optimize VPP [25]. Volumetric printing differs from conventional SLA and CLIP methods by employing multiple intersecting light beams, which facilitate simultaneous polymerization within a 3D volume, as opposed to layer-by-layer construction. For instance, in their alternative method of continuous printing, Walker et al. utilized a mobile fluorinated oil to create a persistent liquid layer beneath the resin. This not only reduced the heat generated during printing but also improved printing performance. With a minimum feature size of 300 μm, the researchers were able to demonstrate a vertical printing speed of 430 mm/h and a volumetric throughput of 100 L/h [26]. In another study, using three superimposing beams to create holographic patterns in light fields, Shusteff et al. created a volumetric 3D printing process that could create 3D structures in a matter of seconds, with a minimum size of approximately 50 μm [27]. This method enhances the printing process efficiency by allowing entire sections of the object to be created in one exposure [28]. Despite its transformational potential, present VPP procedures confront considerable hurdles that demand constant development and innovation. A crucial challenge comes in generating high-resolution prints without sacrificing printing speed. Existing VPP systems generally deal with achieving a balance between resolution and speed, resulting in trade-offs that degrade overall print quality and efficiency [29]. Moreover, VPP techniques usually demand support structures for overhangs and elaborate geometries, introducing complexity and extending post-processing times for print output. Another key problem refers to material qualities and stability, with changes in resin composition, curing times, and ambient conditions resulting in disparities in printed products' mechanical properties and reliability [30]. Furthermore, scalability and cost-effectiveness remain significant problems in VPP, especially with large-scale industrial or commercial applications.

Volumetric printing presents significant promise as an advanced volumetric 3D printing technique [27]. Our previous work on Light Initiated Direct Growth (LIDG) achieved volumetric printing, however, it encounters various challenges that impede its complete realization. A notable concern is energy attenuation as light passes through cured structures, affecting the optical energy required for accurate polymerization in deeper layers [31]. This attenuation requires careful modeling of energy distribution to enhance fabrication efficiency. Furthermore, resin viscosity is crucial; low-viscosity resins may result in unfavorable surface characteristics due to resin flow during exposure, whereas high-viscosity resins require careful formulation to ensure stability [32]. The combination of light intensities, particularly at smaller scales, complicates the attainment of high-resolution prints, as Gaussian distribution effects and pixel blending may result in distortions [33]. Adaptive focusing enhances resolution and promotes uniform growth; however, it complicates energy modeling due to the variability in the optical properties of solid and liquid polymers.

In this study we conducted a thorough analysis of the challenges encountered in LIDG systems, presenting innovative methods to overcome these limitations within the LIDG process utilizing extra inhibition light. The dual-light sources method facilitates precise regulation of the photopolymerization process, permitting the creation of high-resolution and intricate structures without requiring support systems using dynamic projection of orthogonal (both in wavelength and orientation) photoinitiator/inhibition in the XY and YZ planes. This invention may significantly enhance volumetric printing technology, facilitating the production of complex and delicate components with exceptional speed and precision. Additionally, the optimized resin composition aims to minimize variations in material properties and stability, ensuring consistent and reliable performance across printed items. This research demonstrates significant advancements in addressing the limitations of traditional VPP methods and realizing the complete capabilities of continuous 3D printing. The goal is to enhance the adoption of volumetric printing technology across various sectors by addressing significant challenges, including resolution-speed trade-offs, dependence on support systems, material quality, scalability, and cost-effectiveness. volumetric printing is expected to develop into a disruptive manufacturing technology through ongoing innovation and collaboration, driving growth and innovation for the foreseeable future.

The study begins with a comprehensive overview of AM, focusing on its significant influence on conventional production

methods. The discussion shifts to volumetric printing methods, with a particular emphasis on dual-wavelength light-induced direct growth (DW-LIDG) and the necessity of addressing the challenges inherent in this domain to promote innovation. The evolution of literature critic's extensive AM and VPP methods is analyzed, transitioning from traditional layer-by-layer, clip, and volumetric printing to enhance the quality of each method. This analysis defines an extended examination of systems, synthesizing existing research and identifying areas for further research and innovation in the field of DW-LIDG.

2. MATERIALS AND METHODS

2.1 Materials Preparation

The utilization of dual light sources enhances the regulation of resin curing and inhibition. The preparation of materials and methods is crucial for the LIDG process involving light inhibition. It involves specifically formulated resin materials that contain essential compounds, including photo initiators and inhibitors. Systematic protocol of material preparation was employed in this work to enhance material properties and printing conditions, leading to improved quality and reduced production times [34].

The resin preparation process for DW-LIDG is carefully structured to attain the necessary material properties vital for efficient printing. The polymer matrix is prepared by mixing triethylene glycol dimethacrylate (TEGDMA) and bisphenol A glycerolate dimethacrylate (Bis-GMA) in a 1:1 ratio. Catalysts, camphorquinone (CQ) and ethyl 4-dimethylaminobenzoate (EDAB), are also added in a 1:1 weight ratio to initiate polymerization and ensure structural integrity. o-Chloro-4-isocyanatobenzene (o-CI-HABI) is utilized as a photo-inhibitor at a concentration of 1% by weight to regulate polymerization kinetics. A solvent mixture of tetrahydrofuran (THF) and o-CI-HABI is utilized to facilitate the uniform dispersion of resin components, thereby ensuring consistency and homogeneity within the resin. The preparation process includes thorough blending followed by two hours of magnetic stirring for homogeneity. To remove air bubbles and stabilize the resin, the mixture is left undisturbed for 24 hours, allowing trapped air to escape naturally. The above procedures guarantee the resin's preparedness for the following printing process.

2.2 Dual wavelength AM

The optical system of dual-wavelength LIDG was constructed using PDC04-35 projectors, produced by XIAMEN ZHISEN ELECTROMECHANICAL EQUIPMENT CO., LTD, with building area measured 67.2 × 37.8 × 130.0 mm. The projector featured two independent light engines equipped with 458 nm for curing and 365 nm light sources for inhibition. Light intensity at various depths was quantified using a digital light meter (LX1330B, Dr. Meter). A small square of light was directed through the cuvette, ensuring unobstructed passage through the liquid resin without dispersion. The curing light emitted from the projector was concentrated using a convex lens (plano-convex lens (Thorlabs, LA1509-N-BK7, focal length: 100 mm)), and the optical path was redirected from horizontal to vertical via a mirror (first-surface aluminum-coated mirror (Edmund Optics, 43-948, 50.8 mm diameter, 6.35 mm thickness)) for vertical illumination, while the inhibition light directed horizontally through the cuvette. To facilitate the LIDG inhibition process, the resin vat was mounted on a linear stage (404XR, Parker), accommodating up to 400 mL of resin, which accurately simulated real printing conditions. The slicing cross session thickness could be adjusted between 25 and 200 μm. After printing, all objects were rinsed with isopropanol for approximately 30 seconds to remove residual monomers, followed by post-curing for 2 hours to enhance material properties.

3. RESULTS AND DISCUSSION

The employment of a dual-wavelength light source is essential in the proposed design for the LIDG process with inhibitory light. This technique provides exceptional control over the photopolymerization process by employing two distinct wavelengths: blue light at 458 nm for resin curing and ultraviolet (UV) light at 365 nm for inhibition. This configuration facilitates selective photopolymerization, wherein blue light activates polymerization to solidify the resin, but UV light inhibits polymerization in designated regions, hence permitting the creation of intricate geometries without the necessity for support structures. The orthogonal illumination configuration guarantees uniform exposure of the resin, promoting consistent curing and inhibition during the printing process. The dual-wavelength configuration enhances printing attributes, including curing duration and intensity, enabling high-resolution prints with more precision and surface smoothness, while concurrently improving printing speed and efficiency. This configuration reduces print failures while improving overall print reliability and consistency by mitigating prevalent VPP method issues, including overcuring and resin adhesion challenges. Fig. 1a illustrates the dual wavelength photopolymerization setup in detail. The design incorporates two primary light sources: a curing projector that emits blue light at 458 nm and an inhibition projector that emits UV light at 365 nm. The projectors are arranged orthogonally to enable selective control over polymerization and inhibition zones.

The curing light is directed and concentrated through a reflective mirror (45 degree) and convex lens, facilitating precise exposure of the resin in the vat. The perpendicular placement of the inhibition light prevents curing in unintended regions, facilitating the fabrication of intricate geometries. The cuvette, linear stage, and position aligner are essential components that improve the system's precision by assisting dynamic alignment and movement of the resin and light sources. Fig. 1b demonstrates the operational principle of the dual wavelength photopolymerization process. Variation of the projected excitation and inhibition patterns enables the realization of geometric 3D structures in continuous manner. The cuvette holds the resin, which is subjected to curing and inhibition light. The blue light triggers polymerization in designated regions, solidifying the resin, whereas the UV light establishes inhibition

zones, obstructing polymerization in particular areas. Throughout each phase, the resin is subjected to the 458 and 365 nm projector emissions to concurrently regulate polymerization in the XY plane and inhibition in the YZ plane. This selective interaction facilitates the creation of complex structures, including hollow channels and overhanging features, which are difficult to produce using single wavelength enabled LIDG. Furthermore, optimal performance of DW-LIDG is highly dependent on the formulation of the materials used, as shown in Fig. 1c, which delves into the chemistry of the dual-wavelength system. Important photoreactive components included in resin composition include CQ for photoinitiation and o-Cl-HABI for photoinhibition. In contrast to o-Cl-HABI, which selectively inhibits polymerization at 365 nm, 458 nm curing light activates CQ and starts the polymerization process. Polymers like TEGDMA provide the structural basis for the cured material, while co-initiators like EDAB enhance the photoinitiation process so that the printed parts have good resolution, mechanical strength, and uniformity. The real physical printing of 3D object with the light inhibition process is shown in Fig. 1d. It shows how different phases of the printing process with curing light and inhibition light from starting to finishing. By combining curing and inhibition in a single process, it eliminates the need for support structures and enables the creation of intricate geometries, such as overhangs and hollow structures.

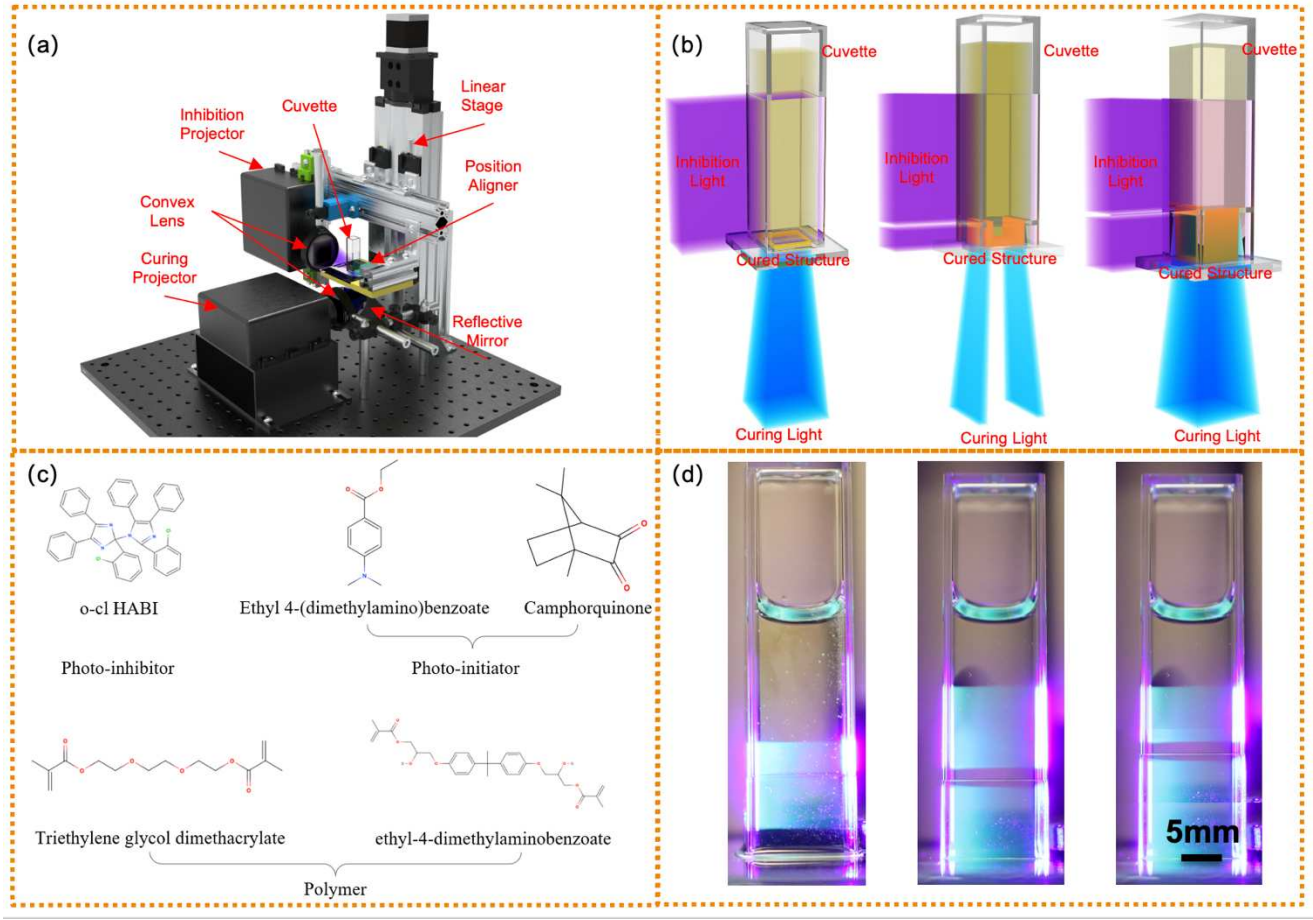

Fig. 1 Schematic illustration of (a) Setup of DW-LIDG with inhibition light; (b) the printing process of 3D object by using DW-LIDG with inhibition light; (c) resin formulation in DW-LIDG; and (d) physical printing process by using DW-LIGG with inhibition light.

The mechanism of DW-LIDG include the interaction between curing and inhibition processes that are fundamental to the system's precision and versatility. Specifically, Fig. 2(a) illustrates that the presence of inhibition light halts photopolymerization. The activation of the photoinitiator by blue light (458 nm) initiates polymerization to form cross-linked networks, while UV light (365 nm) activates the photoinhibitor to selectively inhibit curing. CQ and EDAB function as a visible light photoinitiator and co-initiator, respectively, while o-Cl-HABI acts as a photo-inhibitor. HABIs are recognized as effective photoinitiators when paired with complementary, hydrogen-donating co-initiators. However, in the absence of such co-initiators, the lophyl radicals generated during HABI photolysis inhibit radical-mediated, chain-growth polymerization by rapidly recombining with propagating carbon-centered radicals, thereby preventing polymerization of resin inside the tank [35].

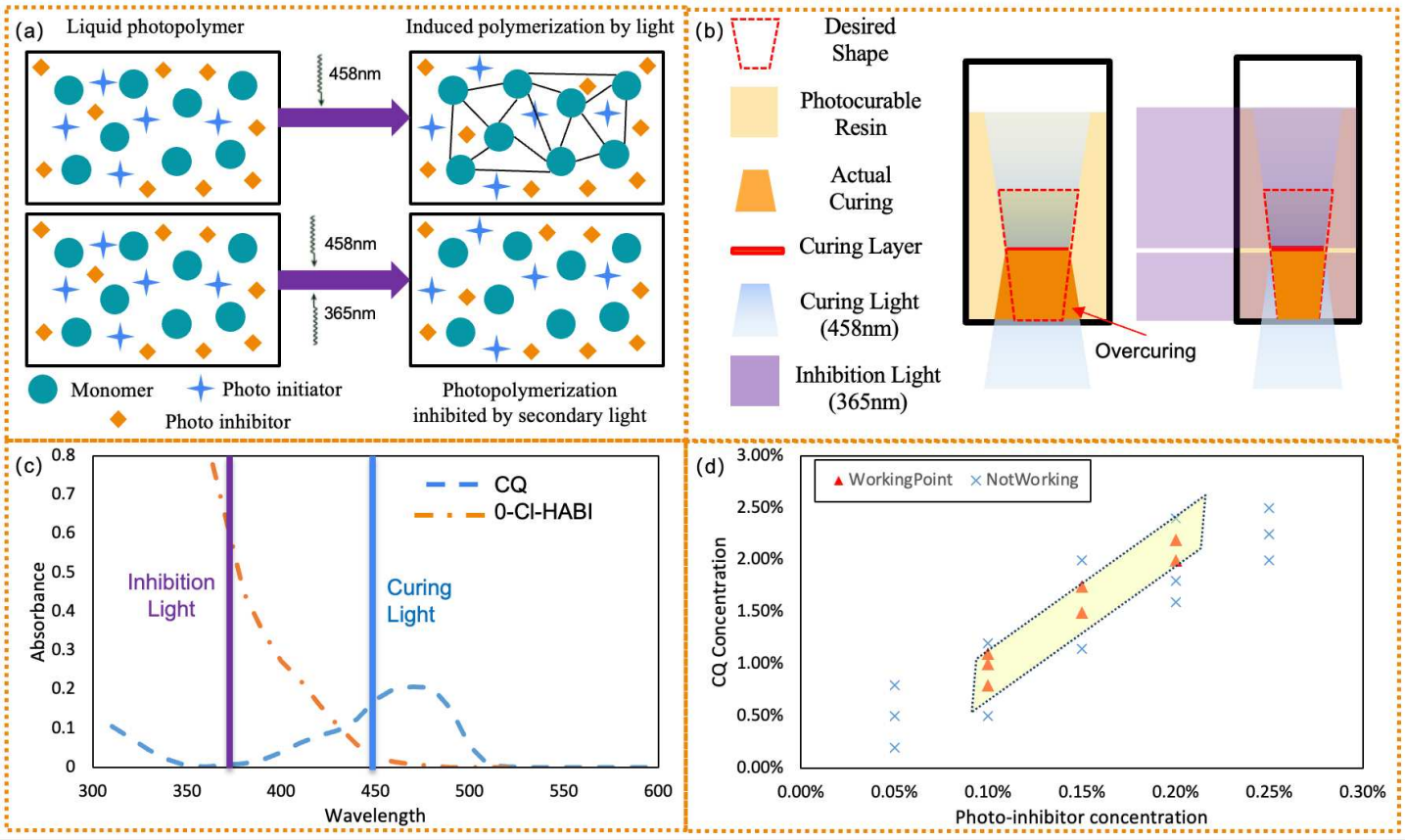

Fig. 2 Schematic illustration of (a) photopolymerization and photo-inhibition; (b) the printing capability of DW-LIDG printing process with inhibition light in concave structure fabrication; (c) molecular absorbance spectrum of photo-initiator CQ and photo-inhibitor o-CI-HABI; and (d) working range for photo-inhibitor and photo-initiator concentrations (the ratio between CQ and EDAB remains the same).

This dual-action method facilitates precise spatial regulation of the polymerization process and the printing capability of concave structures via DW-LIDG is demonstrated in Fig. 2b. When a larger cross-sectional area requires curing on top, the absence of inhibition may result in premature polymerization below the intended position before the photopolymerization of the target area, causing undesirable overcuring features. This occurs due to light scattering and diffusion, which allows the polymerization process to extend beyond the intended region when not properly inhibited. Without spatial confinement, radicals generated during polymerization continue to propagate beyond the curing boundary, leading to excess cross-linking. In LIDG, this effect is particularly pronounced when curing larger cross-sections, as the lack of an inhibitory mechanism allows unintended polymerization below the target session. Implementing an effective photoinhibition system, such as using o-Cl-HABI, helps regulate polymerization kinetics and ensures precise spatial control, preventing overcuring and maintaining structural accuracy [35].

However, the cross area will remain uncured below the target position as long as the inhibition light is applied to that area as illustrated in Fig. 2b. Moreover, orthogonal photoinitiation and photoinhibition necessitate the spectral alignment of the absorbance spectra of the photoinitiator and photo inhibitor with the emission spectra of the light sources. This alignment must ensure that there is no overlap between the output of the photoinitiation source and the absorbance of the photo inhibitor, as well as between the output of the photoinhibition source and the absorbance of the photoinitiator. Both the photoinitiator (CQ) and the photo inhibitor (o-Cl-HABI) play important roles in the dual-wavelength photopolymerization system, and Fig. 2c sheds light on their absorbance spectra. A peak in CQ's absorbance profile at 458 nm corresponds precisely to the wavelength of the blue curing light, allowing for maximum absorption and photo initiator activation to start polymerization. The UV inhibition light selectively activates the photo inhibitor to prevent polymerization in specific locations, and o-Cl-HABI shows significant absorbance near 365 nm, on the other hand. The system's non-overlapping

absorbance peaks ensure accurate spatial control by minimizing cross-reactivity and allowing the lights with two wavelengths to function independently.

To keep the produced structures' high resolution, it is crucial that the curing and inhibition processes not interact with one other. This separation is scientifically critical for printing 3D object via DW-LIDG. It is crucial to fine-tune the resin composition to maximize the reaction of these photoreactive components, as light absorption efficiency at these wavelengths is significant. For example, to achieve maximum light absorption without any undesirable side effects, the concentrations of CQ and o-Cl-HABI need to be carefully calibrated. The capacity to produce tight boundaries between cured and uncured regions is directly translated to the system's precise absorbance behavior. This is important for constructing intricate geometries and complex designs with high accuracy.

Afterwards, we also investigated the correlation between the concentrations of CQ and o-Cl-HABI, finding the sweet spot for effective photopolymerization via DW-LIDG, as shown in Fig. 2d. The green-shaded area on the scatter plot represents the concentrations at which the polymerization and inhibition processes are well-balanced, demonstrating the vital nature of this balance. The red triangles show that the fabrication circumstances were successful, while the blue crosses show that there was either too much or too little polymerization. The working region that accurately formulate resin compositions to obtain dependable results is shown in Fig.2d. From a scientific standpoint, the system's spatial resolution and fidelity are determined by the interaction between CQ and o-Cl-HABI concentrations. To commence robust polymerization and build a solid, well-defined structure, CQ, which is triggered by blue light (458 nm), needs to be present in adequate concentrations. Overcuring, caused by an excess of CQ, can cause boundaries to become blurry, while if the concentration is less than expected value, structural information will be lost. It is also important to maintain a steady concentration of o-Cl-HABI, which is triggered by UV light at 365 nm, such that it does not entirely stop polymerization but does limit cure in undesirable areas. Too much o-Cl-HABI in the solution can prevent polymerization even in the targeted curing zones, which will lead to structural failure. To keep this fine equilibrium, the concentrations of CQ and o-Cl-HABI must be proportionate, as seen by the s working zone on the plot of Fig.2d. This range is critical for the DW-LIDG system's operation at high spatial resolution, which allows for the defect-free fabrication of complicated shapes. Findings from this study demonstrate the scientific precision required in formulating resin compositions, as deviations from the optimal range disrupt the delicate balance between curing and inhibition, resulting in reduced accuracy and efficacy.

Following the analysis of inhibition characteristics, it is critical to evaluate the curing behavior under two distinct conditions: with and without inhibition light. Curing without inhibition light involves using a single curing light source, whereas curing with inhibition entails illuminating the entire resin tank with inhibition light, excluding the area undergoing photopolymerization. All tests were conducted through continuous printing with the resin tank moving steadily along the z-axis to prevent blurring or defocusing of the curing light. The curing heights obtained for various curing times, conditions, and curing lights at different grayscale levels are presented in Fig. 3a. The results clearly demonstrate that, in the absence of inhibition light, the curing height increases rapidly across all grayscale values, with the highest grayscale level (255) yielding the quickest curing rate. This observation is attributed to higher grayscale levels corresponding to greater light intensities and deeper penetration depths, thus enhancing photoinitiator activation and accelerating polymerization. In contrast, introducing inhibition light substantially reduces the curing growth rate, particularly at lower grayscale levels (e.g., 50 and 100). However, the overall reduction in growth rate due to inhibition is not markedly greater than the inherent differences observed among various grayscale levels. This behavior results from the photo inhibitor activation, which competes with the photoinitiator and suppresses polymerization in non-target regions.

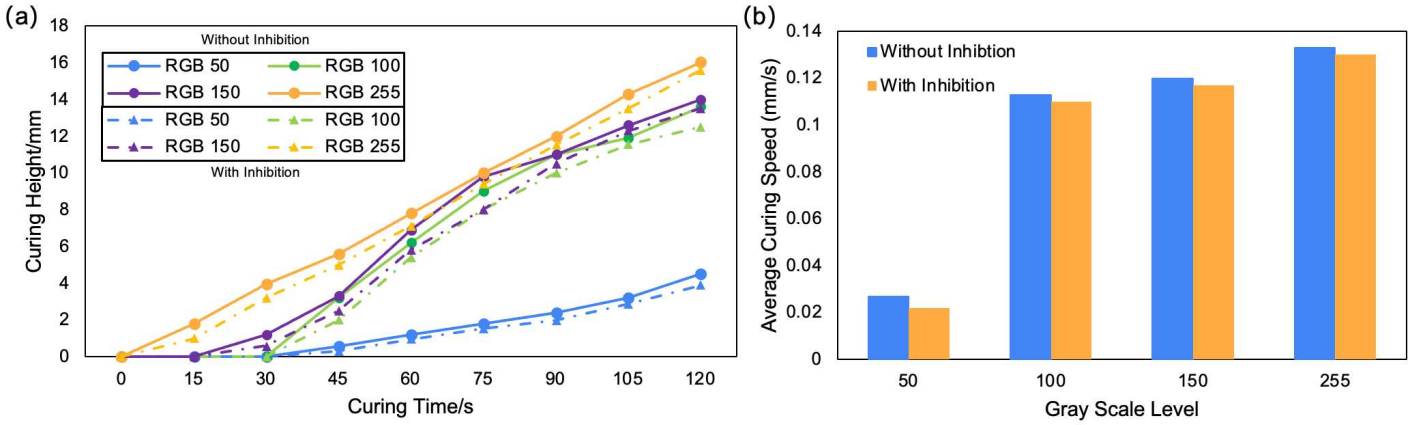

Fig. 3 (a) Curing height vs time uder different gray scale levels with/without inhibition light; and (b) average curing speeds at different gray scale levels with/without inhibition light.

Moreover, Fig. 3b illustrates the effect of inhibition on curing speed as a function of grayscale intensity. The cure velocity sharply increases with elevated grayscale values, reaching its maximum at 255. However, the introduction of inhibition uniformly reduces the curing rate across all grayscale intensities. This inhibitory layer significantly moderates the curing process by establishing competitive interactions between curing and inhibition mechanisms, thereby enhancing precision in depth control. The data in both figures emphasize a critical balance between light intensity and inhibition: higher intensities accelerate curing, while the inhibitory mechanism provides an essential regulatory control to moderate the polymerization process. This scientific insight is particularly relevant, as it allows precise customization of curing depth and velocity—an essential factor for fabricating complex structures with high fidelity.

These findings highlight the capability of the dual-wavelength system to finely control curing dynamics through inhibition. By reducing cure rates, the inhibitory effect is particularly beneficial in applications requiring high spatial resolution, such as microfluidic devices or intricate geometries, where excessive polymerization could compromise structural accuracy. Thus, this technology enhances the fabrication process by optimizing the interplay between curing and inhibition, reducing defects, and increasing precision in advanced manufacturing applications.

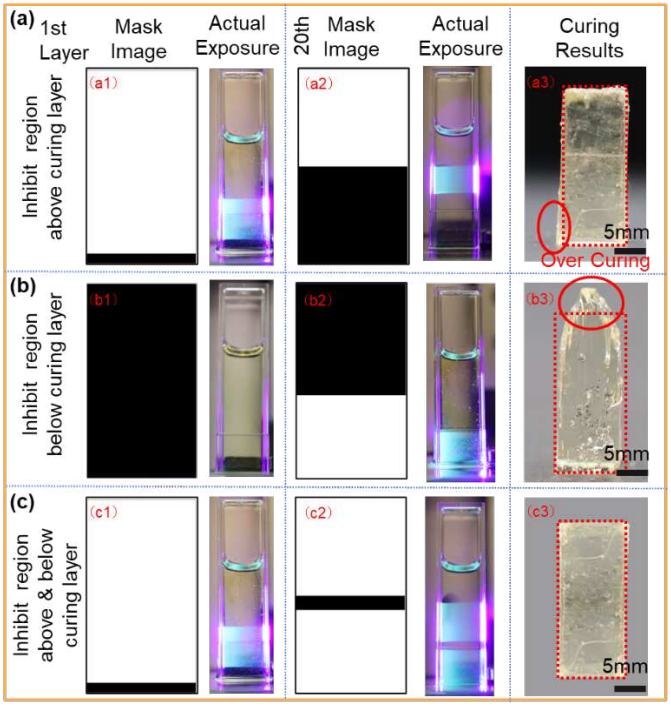

Fig. 4 Comparison of printing results using the inhibition curing light with different patterns (a) inhibition region above curing layer; (b) inhibition region below the curing layer; and (c) inhibition region above & below the curing layer.

Upon understanding the inhibition and curing characteristics, it becomes essential to develop and evaluate a printing process for LIDG incorporating inhibition light. Three distinct printing methods using inhibition light are proposed and illustrated in Fig. 4. In the first method, inhibition light is applied exclusively above the curing layer. In the second method, inhibition is implemented solely below the curing layer. The third method involves applying inhibition light both above and below the curing layer simultaneously. Each process was tested by fabricating 20 mm-high cuboid structures with a 10 × 10 mm square base. All three methods utilized identical curing lights, differing only in the placement of inhibition illumination.

In the first scenario, where the inhibition layer is positioned above the curing layer, the mask images and actual exposure confirm that UV radiation (365 nm) effectively creates an inhibition zone at the top, preventing polymerization above the curing zone. Nevertheless, the curing results (Fig. 4a3) show evidence of overcuring at the peripheries, particularly near the upper boundary. This occurs because the inhibitory layer restricts polymerization only from above, leaving the lower boundary unregulated, allowing curing light to penetrate beyond the intended region. In the second scenario, with the inhibition region placed below the curing layer, the mask images and actual UV exposure effectively prevent polymerization beneath the curing zone. The resulting structures (Fig. 4b3) exhibit significantly improved control compared to Fig. 4a3, showing reduced overcuring at the lower boundary. However, due to the absence of an inhibitory layer above, slight deviations remain at the upper boundary caused by unrestricted curing light penetration. The third method, involving inhibition layers both above and below the curing region, is anticipated to yield optimal results. Mask images (Fig. 4c1, c2) and actual UV exposure validate precise boundary limits at both the upper and lower regions. The resulting cured structure (Fig. 4c3) exhibits superior spatial control, featuring sharply defined edges and minimal overcuring. This configuration represents the most precise polymerization, as the dual inhibition zones restrict unwanted curing light penetration, ensuring that the cured layer closely conforms to the intended design.

These findings highlight the critical role of inhibition zones in precisely regulating polymerization boundaries and preventing overcuring. When inhibition is applied exclusively to either the upper or lower region (as in Fig.4a and b), the unprotected boundary remains susceptible to curing light penetration, resulting in deviations from the intended structure. The dual-wavelength approach achieves optimal spatial control by simultaneously applying inhibition layers on both sides (Fig.4c), thus precisely delineating cured and uncured regions. Such accurate spatial control is scientifically significant for applications requiring high-resolution manufacturing and defect-free components. Furthermore, this dual-wavelength technology eliminates the necessity for post-processing corrections, enhancing both efficiency and structural fidelity in advanced photopolymerization processes.

Finally, three structures—(a) a spear and rack, (b) the ASU logo, and (c) a square block featuring a hollow section—were

successfully printed using the DW-LIDG process with inhibition light, as shown in Fig. 5. The standard inhibition approach, described previously, was employed for these demonstration prints. All printed structures showed no significant signs of overcuring or undercuring. The superior printing quality ensured precise alignment between the spear and rack components, enabling smooth rotational motion of the spear as intended.

When volumetric printing was initially introduced as a rapid, single-step fabrication technique, it was limited primarily to simple geometries. Creating more complex structures required either multiple photoinitiation sources aligned along all three spatial dimensions or a rotating resin container illuminated by sequential patterns [36]. By employing orthogonally positioned projectors within a dual-wavelength approach, combining photoinitiation and photoinhibition, this work advances the capability to fabricate structures with significantly higher geometric complexity—structures that are impossible to produce using LIDG with single wavelength. Through the dynamic coordination of projector outputs at 365 nm and 458 nm, a 365 nm irradiation pattern was applied from the side to define polymerizable and non-polymerizable zones, while a complementary 473 nm pattern established the precise cross-linking geometry within the polymerizable region. Utilizing dual-wavelength illumination provides a versatile and effective strategy for the LIDG process enhanced by inhibitory control, resulting in exceptional spatial precision during photopolymerization.

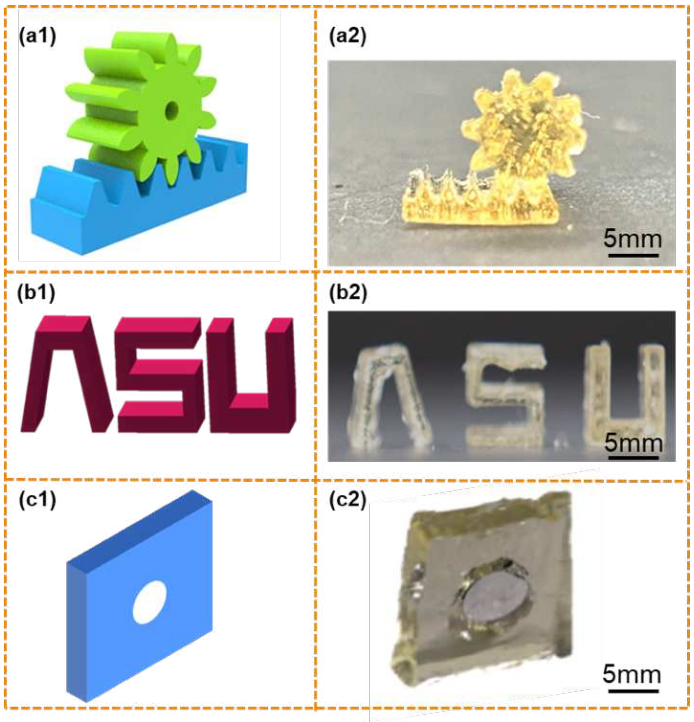

Fig. 5 Demonstration printing of (a) gear and rack; (b) ASU; and (c) square block with hollow section (1) CAD model; (2) DW-LIDG printed part.

4. CONCLUSION AND FUTURE WORK

In summary, our investigation into dual-wavelength volumetric printing (DW-LIDG) presented a significant progression in single step AM. In our research, we systematically identified and addressed challenges inherent LIDG, proposing innovative solutions to mitigate these limitations. We have achieved high accuracy and control over the photopolymerization process by integrating a light source system with two wavelengths, enabling the fabrication of complex structures without requiring intricate support materials. Additionally, our efforts necessitated meticulous optimization of the resin formulations, involving the precise selection of photoinitiators, co-initiators, and photoinhibitors. While its application in large-scale manufacturing requires careful evaluation of energy usage, equipment intricacy, and material expenses. This approach led to significant improvements in print speed and complexity compared with single wavelength LIDG. Our methodology, defined by a stringent resin production protocol and comprehensive experimental validation, demonstrates the efficacy of our strategy in addressing current challenges and facilitating the advancements of DW-LIDG technology. These developments enhance scholarly discourse on volumetric printing techniques and establish a foundation for their practical application across various industries. The ongoing refinement and expansion of our findings indicate that the future development of DW-LIDG technology is likely to yield significant innovations and enhance operational efficiency, potentially transforming conventional manufacturing processes. We anticipate that sustained investment in research and development will significantly enhance production, resulting in improved performance and technological progress.

Further research avenues beckon, inviting exploration into the nuanced optimization of printing parameters and material formulations. Delving deeper into the technology's scalability for industrial deployment and probing into uncharted application, like biomedical engineering and optics, promise to unveil new dimensions of its potential. Overall, DW-LIDG could redefine the very fabric of single step additive manufacturing, ushering in an era of unparalleled efficiency and creativity across polymer fabricaiton industries.

ACKNOWLEDGEMENTS

The authors acknowledge ASU Startup Funding, ASU FSE Strategic Interest Seed Funding NEI-STC-MADE grant, National Science Foundation (NSF grant No. CMMI-2114119, 2338752).

REFERENCES

[1] Gouttebroze, S., et al. “Toward Semantic Standard and Process Ontology for Additive Manufacturing.” IOP Conference Series: Materials Science and Engineering, vol. 1281, no. 1, 2023, p. 012014, https://doi.org/10.1088/1757-899x/1281/1/012014.

[2] Gibson, Ian, et al. “Additive Manufacturing

Technologies." Additive Manufacturing Technologies, 2020, pp. 1–675, https://doi.org/10.1007/978-3-030-56127-7.

[3] Calignano, Flaviana, et al. "Overview on Additive Manufacturing Technologies." Proceedings of the IEEE, vol. 105, no. 4, 2017, pp. 593–612, https://doi.org/10.1109/JPROC.2016.2625098.

[4] Tofail, Syed A. M., et al. "Additive Manufacturing: Scientific and Technological Challenges, Market Uptake and Opportunities." Materials Today, vol. 21, no. 1, 2018, pp. 22–37, https://doi.org/10.1016/j.mattod.2017.07.001.

[5] Campbell, Ian, et al. "Additive Manufacturing: Rapid Prototyping Comes of Age." Environment and Planning A, vol. 41, 2013, pp. 1366–85.

[6] Khan, Numan, and Aniello Riccio. "A Systematic Review of Design for Additive Manufacturing of Aerospace Lattice Structures: Current Trends and Future Directions." Progress in Aerospace Sciences, vol. 149, no. April, 2024, p. 101021, https://doi.org/10.1016/j.paerosci.2024.101021.

[7] Radhika, C., et al. "A Review on Additive Manufacturing for Aerospace Application." Materials Research Express, vol. 11, no. 2, 2024, https://doi.org/10.1088/2053-1591/ad21ad.

[8] Sun, Yage, et al. "3D-Printed, Bi-Layer, Biomimetic Artificial Periosteum for Boosting Bone Regeneration." Bio-Design and Manufacturing, vol. 5, no. 3, 2022, pp. 540–55, https://doi.org/10.1007/s42242-022-00191-6.

[9] Wang, Xiaocheng, et al. "3D-Printed Tissue Repair Patch Combining Mechanical Support and Magnetism for Controlled Skeletal Muscle Regeneration." Bio-Design and Manufacturing, vol. 5, no. 2, 2022, pp. 249–64, https://doi.org/10.1007/s42242-021-00180-1.

[10] Xu, Heqi, et al. "Cell Sedimentation during 3D Bioprinting: A Mini Review." Bio-Design and Manufacturing, vol. 5, no. 3, 2022, pp. 617–26, https://doi.org/10.1007/s42242-022-00183-6.

[11] Bassoli, Elena, et al. "Design for Additive Manufacturing and for Machining in the Automotive Field." Applied Sciences (Switzerland), vol. 11, no. 16, 2021, https://doi.org/10.3390/app11167559.

[12] Vasco, Joel C. "Chapter 16 - Additive Manufacturing for the Automotive Industry." Handbooks in Advanced Manufacturing, edited by Juan Pou et al., Elsevier, 2021, pp. 505–30, https://doi.org/https://doi.org/10.1016/B978-0-12-818411-0.00010-0.

[13] Esteve, Felip, et al. Micro-Additive Manufacturing Technology BT - Micro-Manufacturing Technologies and Their Applications: A Theoretical and Practical Guide. Edited by Irene Fassi and David Shipley, Springer International Publishing, 2017, pp. 67–95, https://doi.org/10.1007/978-3-319-39651-4_3.

[14] Fidan, Ismail, et al. "Nano-Level Additive Manufacturing: Condensed Review of Processes, Materials, and Industrial Applications." Technologies, vol. 12, no. 7, 2024, https://doi.org/10.3390/technologies12070117.

[15] Huang, Zhiyuan, et al. "Micro/Nano Functional Devices Fabricated by Additive Manufacturing." Progress in Materials Science, vol. 131, no. July 2022, 2023, p. 101020, https://doi.org/10.1016/j.pmatsci.2022.101020.

[16] Kafle, Abishek, et al. "3d/4d Printing of Polymers: Fused Deposition Modelling (Fdm), Selective Laser Sintering (Sls), and Stereolithography (Sla)." Polymers, vol. 13, no. 18, 2021, pp. 1–37, https://doi.org/10.3390/polym13183101.

[17] Abdulhameed, Osama, et al. "Additive Manufacturing: Challenges, Trends, and Applications." Advances in Mechanical Engineering, vol. 11, no. 2, 2019, pp. 1–27, https://doi.org/10.1177/1687814018822880.

[18] Lehmann, Thomas, et al. "Large-Scale Metal Additive Manufacturing: A Holistic Review of the State of the Art and Challenges." International Materials Reviews, vol. 67, no. 4, 2022, pp. 410–59, https://doi.org/10.1080/09506608.2021.1971427.

[19] Joralmon, Dylan, et al. "Continuous 3D Printing of Metal Structures Using Ultrafast Mask Video Projection Initiated Vat Photopolymerization." Additive Manufacturing, vol. 89, no. February, 2024, p. 104314, https://doi.org/10.1016/j.addma.2024.104314.

[20] Methani, Mohammed M., et al. "Additive Manufacturing in Dentistry: Current Technologies, Clinical Applications, and Limitations." Current Oral Health Reports, vol. 7, no. 4, 2020, pp. 327–34, https://doi.org/10.1007/s40496-020-00288-w.

[21] Zhou, Longfei, et al. "Additive Manufacturing: A Comprehensive Review." Sensors, vol. 24, no. 9, 2024, https://doi.org/10.3390/s24092668.

[22] Lipkowitz, Gabriel, et al. "Injection Continuous Liquid Interface Production of 3D Objects." Science Advances, vol. 8, no. 39, 2022, pp. 1349–52, https://doi.org/10.1126/sciadv.abq3917.

[23] Balli, Judah, et al. Continuous Liquid Interface Production of 3D Objects: An Unconventional Technology and Its Challenges and Opportunities. 3 Nov. 2017, https://doi.org/10.1115/IMECE2017-71802.

[24] Kowsari, Kavin, et al. “Photopolymer Formulation to Minimize Feature Size, Surface Roughness, and Stair-Stepping in Digital Light Processing-Based Three-Dimensional Printing.” Additive Manufacturing, vol. 24, no. October, 2018, pp. 627–38, https://doi.org/10.1016/j.addma.2018.10.037.

[25] Whyte, Daniel J., et al. “Volumetric Additive Manufacturing: A New Frontier in Layer-Less 3D Printing.” Additive Manufacturing, vol. 84, no. September 2023, 2024, p. 104094, https://doi.org/10.1016/j.addma.2024.104094.

[26] Walker, David A., et al. “Rapid, Large-Volume, Thermally Controlled 3D Printing Using a Mobile Liquid Interface.” Science, vol. 366, no. 6463, Oct. 2019, pp. 360–64, https://doi.org/10.1126/science.aax1562.

[27] Shusteff, Maxim, et al. “One-Step Volumetric Additive Manufacturing of Complex Polymer Structures.” Science Advances, vol. 3, no. 12, 2017, https://doi.org/10.1126/sciadv.aao5496.

[28] Thijssen, Quinten, et al. “From Pixels to Voxels: A Mechanistic Perspective on Volumetric 3D-Printing.” Progress in Polymer Science, vol. 147, 2023, p. 101755, https://doi.org/10.1016/j.progpolymsci.2023.101755.

[29] Zhao, Lidong, et al. “Limiting Defect in Vat Photopolymerization via Visual-Guided in-Situ Repair.” Additive Manufacturing, vol. 79, no. September 2023, 2024, p. 103947, https://doi.org/10.1016/j.addma.2023.103947.

[30] Paral, Sandeep Kumar, et al. “A Review of Critical Issues in High-Speed Vat Photopolymerization.” Polymers, vol. 15, no. 12, 2023, https://doi.org/10.3390/polym15122716.

[31] Lin, Wei, et al. “Emerging Micro-Additive Manufacturing Technologies Enabled by Novel Optical Methods.” Photonics Research, vol. 8, no. 12, 2020, p. 1827, https://doi.org/10.1364/prj.404334.

[32] Shusteff, Maxim, et al. “Volumetric Additive Manufacturing of Polymer Structures by Holographically Projected Light Fields. ” no. 2001, 2017.

[33] Zhang, Feng, et al. “The Recent Development of Vat Photopolymerization: A Review.” Additive Manufacturing, vol. 48, no. October, 2021, https://doi.org/10.1016/j.addma.2021.102423.

[34] Ngo, Tuan D., et al. “Additive Manufacturing (3D Printing): A Review of Materials, Methods, Applications and Challenges.” Composites Part B: Engineering, vol. 143, 2018, pp. 172–96, https://doi.org/https://doi.org/10.1016/j.compositesb.2018.02.012.

[35] Li, Feng, et al. “Rapid Additive Manufacturing of 3D Geometric Structures via Dual-Wavelength Polymerization.” ACS Macro Letters, vol. 9, no. 10, 2020, pp.1409–14, https://doi.org/10.1021/acsmacrolett.0c00465.

[36] Kelly, Brett E., et al. “Volumetric Additive Manufacturing via Tomographic Reconstruction.” Science, vol. 363, no. 6431, 2019, pp. 1075–79, https://doi.org/10.1126/science.aau7114.